

Alma Mater Studiorum Università di Bologna
Archivio istituzionale della ricerca

Vibroacoustic analysis of an innovative windowless cabin with metamaterial trim panels in regional turboprops

This is the final peer-reviewed author's accepted manuscript (postprint) of the following publication:

Published Version:

Moruzzi, M.C., Cinefra, M., Bagassi, S. (2021). Vibroacoustic analysis of an innovative windowless cabin with metamaterial trim panels in regional turboprops. *MECHANICS OF ADVANCED MATERIALS AND STRUCTURES*, 28(14), 1509-1521 [10.1080/15376494.2019.1682729].

Availability:

This version is available at: <https://hdl.handle.net/11585/708152> since: 2019-12-12

Published:

DOI: <http://doi.org/10.1080/15376494.2019.1682729>

Terms of use:

Some rights reserved. The terms and conditions for the reuse of this version of the manuscript are specified in the publishing policy. For all terms of use and more information see the publisher's website.

This item was downloaded from IRIS Università di Bologna (<https://cris.unibo.it/>).
When citing, please refer to the published version.

(Article begins on next page)

Vibroacoustic analysis of an innovative windowless cabin with metamaterial trim panels in regional turboprops

M. C. Moruzzi¹, M. Cinefra¹, S. Bagassi²

(1) Department of Mechanical and Aerospace Engineering, Politecnico di Torino, Italy

(2) Department of Industrial Engineering, Università di Bologna, Italy

Keywords:

Metamaterial, Finite Element Method, Vibroacoustic analysis, Noise reduction, Sound pressure level, Cabin comfort.

Author and address for Correspondence

Prof. Maria Cinefra

Associate Professor,

Department of Mechanical and Aerospace Engineering

Politecnico di Torino,

Corso Duca degli Abruzzi, 24,

10129 Torino, ITALY,

tel +39.011.090.6845, fax +39.011.090.6899

e.mail: maria.cinefra@polito.it

Abstract

The purpose of this work is to study the possible noise reduction, in terms of sound pressure level, in the passenger cabin of a regional turboprop aircraft under multiple tonal and broadband noise components characterizing the noise generated by the engines during cruise flight conditions. In particular, we want to show the acoustic performances of innovative passive Noise & Vibration technologies, such as acoustic metamaterials applied to the trim panel of the cabin, in the low frequency range, from 100 Hz to 300 Hz. Moreover, the removal of windows from the passenger cabin is evaluated, in acoustic terms. Analyses are performed using a numerical tool, Actran, a finite element based software, and a numerical model of a regional aircraft fuselage. According to the results, metamaterials seem to have significant acoustic performances that lead to a reduction in noise and therefore an increase in passenger comfort.

1 Introduction

The aim of this work is to evaluate new technologies and configurations, to reduce the sound pressure level in the passenger cabin of a turboprop regional aircraft, in order to achieve improvement in noise reduction and in passenger comfort, according to the studies by Sir Rayleigh [1] and Beranek [2], especially referring to low frequency noise. In particular, we want to evaluate the acoustic efficiency of using metamaterials for the trim panel. Moreover the possible acoustic advantages of a windowless configuration are studied.

In the aeronautic sector, no regulations exist for internal noise, but they do for external noise. The requirements are driven by costumer need, identified by the marketing analysts, and by the passenger and crew safety. Instead, the vibration and the noise of the cockpit equipment must not interfere with safe operation of the aircraft, allowing safe and clear communication between the pilots and the crew; moreover noise must not cause distraction. Finally, there are military regulations, concerning internal noise, but they refer to the noise exposure hazards in the aircraft cabin and speech clarity. The latter military regulations are discussed by Beranek [3]. As reference value, cabin pressure level, for passenger aircrafts, must be between 60 and 88 dB. A long exposure to a pressure level of 85 dB could cause hearing loss, fatigue and reduction of concentration, not only for the passenger but also the crew. An overview of auditory and non-auditory effects of noise on health are reported in the work of Basner et al. [4].

The acoustic treatments, understood as means/technical solutions that are installed on board, to increase noise reduction through the fuselage wall and to control internal noise sources, are described in the paper by Nichols et al. [5]. Some technologies proposed in the past are resumed in the work by Dobrzynski [6]. The following items contribute to reduce internal noise levels and hence may be regarded as noise treatments: thermo-acoustic blankets, skin damping, furnishing panels, mufflers, active noise control systems. The acoustic treatments configuration needs to be optimized taking into account different parameters, particularly weight and cost; an example is given by the honeycomb acoustic metamaterial proposed by Sui et al. [7], which possesses lightweight and yet sound-proof properties. In particular, if one refers to a regional turboprop it can be considered that the mass of fuselage blankets, in percentage of the MEW (manufacturer's empty weight), should be less than 1.4%. For these reasons, acoustic metamaterials are used as acoustic solution in this work.

In the last decade, a new research field has emerged to study metamaterials [8]. This term refers to materials whose properties are "beyond" those of conventional materials. In this work, we consider acoustic metamaterials composed of a host viscoelastic material with high-density inclusions. The constituent materials can include composite materials, metals, foams or plastics. The core concept of metamaterial

is to replace the molecules with man-made structures called unit cell. They can be viewed as artificial atoms, usually arranged in repeating patterns on a scale much less than the relevant wavelength of the phenomena they influence. Several types of metamaterials were studied: electromagnetic metamaterials [9, 10, 11, 12] and mechanical metamaterials [13, 14, 15]. The acoustic metamaterials (AMMs) have the same paradigm of their electromagnetic relatives. In fact they try to regulate acoustic behavior, resulting in negative effective mass density and negative effective bulk modulus based on localized resonance mechanisms and dispersion properties [16]. Furthermore AMMs, due to negative mass density, demonstrate excellent performance at low frequencies, as described in [17, 18, 19]. In this work we use the AMM proposed by D’Amico et al. [20], that consist in a melamine foam plate pierced with cylindrical aluminum inclusions, Fig. 1. In this work, the authors calculated the homogenized mechanical and inertial properties of the metamaterial and evaluated its acoustic performances in terms of transmission loss.

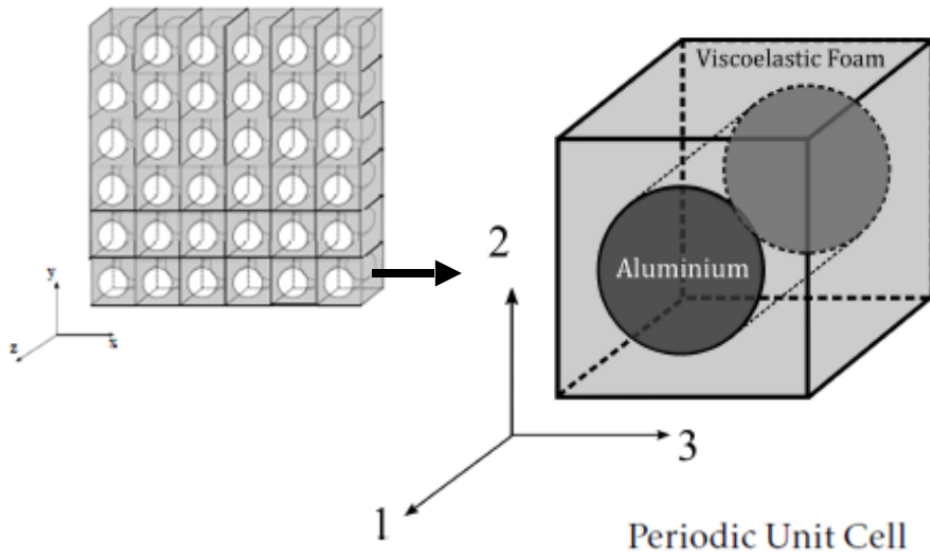


Figure 1: Metamaterial studied by D’Amico et al. [20] with different inclusions (300 and 600) and the homogenized material.

In literature, studies on acoustic cavity have been widely conducted in the automotive field, as presented by Yuksel et al. [21] and by Accardo et al. [22]. In the aeronautic field, relating to acoustic analysis on the passenger cabin, we refer to the works of Passabì et al. [23] and of Cinefra et al. [24]. In the first paper, the analysis concentrates on a section of the passenger cabin, with a monopolar acoustic source; in the second work, an acoustic analysis on a complete passenger cabin is performed through a Statistical Energy Analysis (SEA). Furthermore, the use of models to integrate innovative material, as composites and metamaterials, was performed by the work of Franco et al. [25], Petrone et al. [26], Arunkumar et al. [27] and D’Alessandro et al. [28] for sandwich plates and in general composite materials and of Cutanda Henriquez et al. [29] for metamaterials, both for theoretical models and numerical modeling, with experimental testing supporting these models in [28]. All these works demonstrate that the availability of a numerical tool, especially for regional aircrafts subject to very different customer requests, is a fundamental need together with the confidence of the users of such tools who should have the ability to correctly and realistically interpret the numerical results produced by the chosen tool. The basic assumptions rely on the diffuse acoustic field inside each elemental volume and on the acoustic energy balance among the input source and the exchange output among the different volumes. In parallel,

the possibility of studying different materials is a driving factor for approaching the problem of aircraft interior noise.

This paper will present the results obtained by numerical simulations performed with Actran. Actran (acoustic transmission) is finite element based software developed by the Free Field Technologies, MSC Software Company, for acoustic, vibroacoustic and aeroacoustic analysis. Actran provides a rich library of material models, a complete elements library and high performance solvers. Actran has been chosen because it allows to define boundary conditions and materials with frequency dependent characteristics, as metamaterials. Moreover, Actran allows to study materials with unconventional properties, as porous or viscoelastic materials.

Combined with a strong acoustic model, we need a way to define the acoustic source in the selected range of frequency. For low frequencies, on a turboprop aircraft, near field excitation is mainly due to the propeller and therefore the major part of the acoustic energy is concentrated in the low frequency range (0-300 Hz), although for last generation turboprop aircraft, the near field noise excitation is also due to turbulent boundary layer. Furthermore there could be a resonance between natural frequencies of the skin panel and the propeller tone frequencies, that increases noise transmission, as explained by Cinefra et al [24]. In our work, we focus on noise generated by the propellers, while the noise due to the turbulent boundary layer was studied in [24].

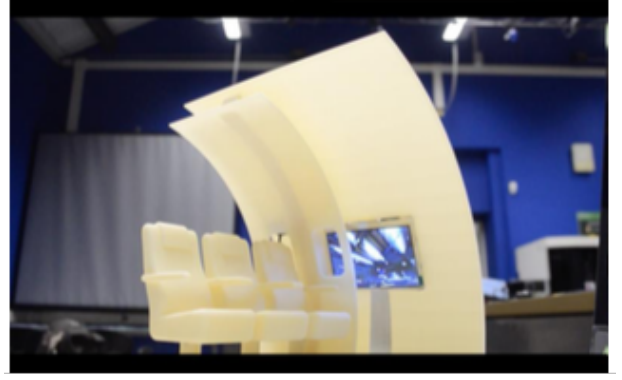
In the framework of the vibroacoustic analysis of the cabin cavity, the innovative concept of 'windowless' fuselage has also been assessed. This concept consists in a passenger aircraft fuselage without windows, in which windows are replaced by monitors connected to external cameras (model of false windows with monitor in Fig. 2 developed by Bagassi et al. [30]). The windowless concept has been studied in literature through three different configurations:

- windowless cockpit as described by Berth et al. [31] and by Zaneboni et al. [32];
- windowless fuselage used on blended wing body aircraft in the works of Liebeck [33] and of Van Der Voet et al. [34];
- windowless fuselage in traditional passenger aircrafts, in the works of Bagassi et al. [35] for short-medium range aircrafts and [36] for long range aircrafts.

The first case consists in removing the windscreens: besides the weight reduction, there is better pressure distributions on the aircraft bow. The windscreens are replaced with monitors and cameras to guarantee a 360° view. On a blended wing body aircraft it is impossible, because of the particular shape of the wing-fuselage structure, to have windows and exits. Therefore, solutions to limit passenger discomfort deriving from a windowless cabin in future commercial blended wing body aircraft should be considered. In a traditional fuselage exploiting a windowless design, all windows, except those of emergency exits, are removed and replaced with a visual system, composed by internal monitors and external cameras. In particular, this last configuration could be applied to a traditional short-medium aircraft and it is considered in this work. The main objective of this concept is to achieve a lighter aircraft, because removing windows leads to a reduction in weight (windows are holes in the structure and they need reinforcements). Actually, a lighter aircraft consumes less fuel and produces lower emissions. Another possible advantage is the reduction of noise in the passenger cabin and it will be investigated in this work.



(a)



(b)

Figure 2: small scale model of false windows.

2 FEM model

2.1 Geometry and mesh quality

The aircraft model, based on FEM (Finite Element Method), is a baseline fuselage, used to demonstrate the effectiveness of the acoustic solutions at low frequencies. The purpose is to create a system that reproduces the dynamic behavior of the real structure in terms of mechanical impedance and coupling between the fuselage airframe and the fluid within it. The FEM model is composed by 0D, 1D, 2D and 3D elements. The external shells and the passenger cabin are reported in Fig. 3 and Fig. 4 respectively.

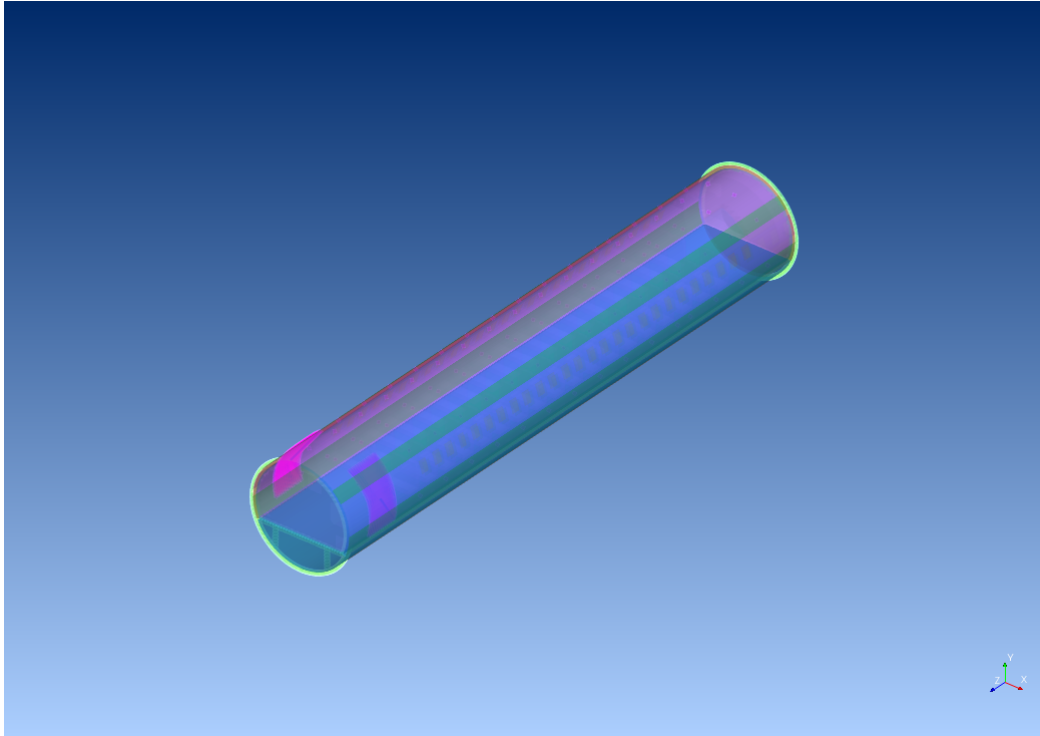


Figure 3: Model of the skin and cavities: 2D and 3D elements.

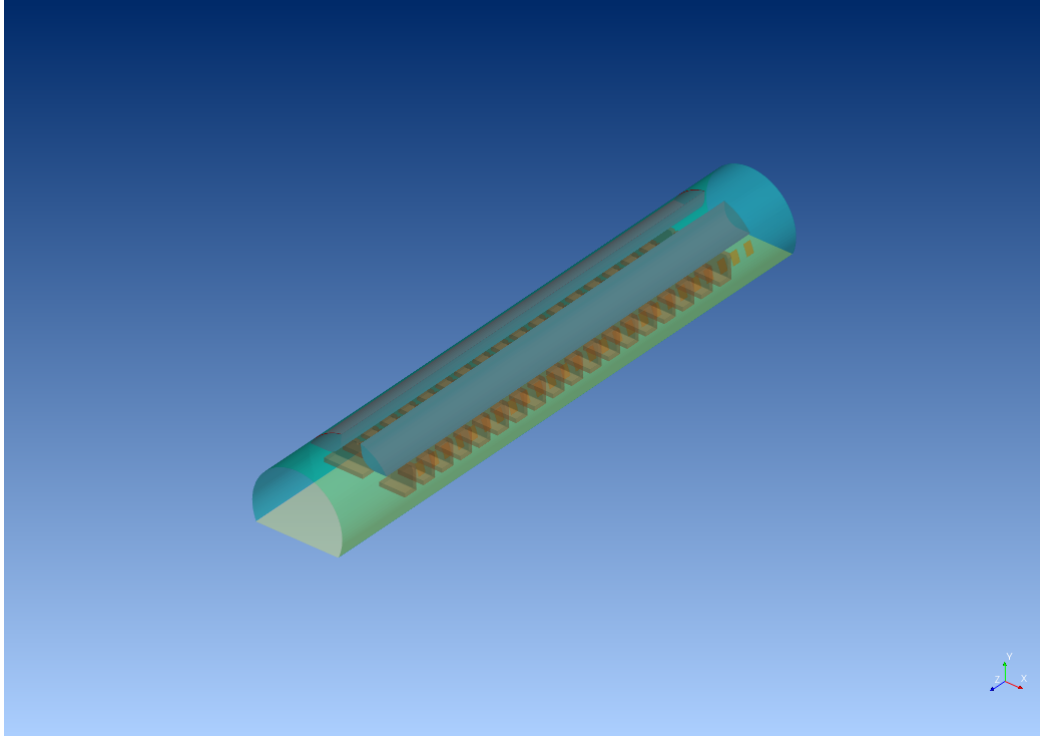


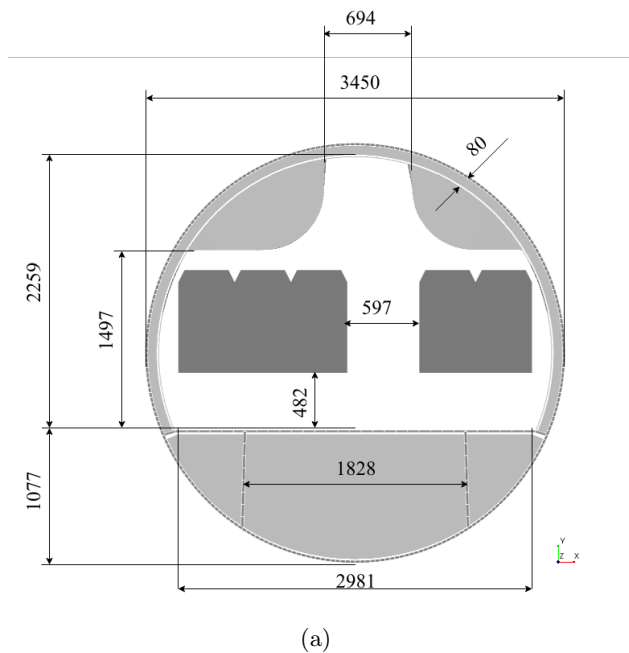
Figure 4: passenger cabin with trim panel, overheads, floor and seats.

The model represents an aircraft with a length of 19.88 m, an external diameter of 3.45 m and a passenger cabin height of 2.26 m. The model's dimensions are reported in Fig. 5(a) and Fig. 5(b). The window sizes are reported in Fig. 6 and the seats sizes in Fig. 7.

Mesh is composed by 0D, 1D, 2D and 3D elements, with linear interpolation, except the trim panel, that has elements with a quadratic interpolation because it is a tridimensional orthotropic metamaterial. Linear interpolation has less computational cost, but requires a wavelength criterion of at least 7 elements per wavelength, while a quadratic a wavelength criterion of 3. The total number of elements is equal to 1291973 (created in the analysis 1481150), the degrees of freedom of the problem to 2246063 and the topological dimension to 3. Element types and dimensions are reported in Fig. 8. The element distribution through the different components is reported in Fig. 9. It is possible to see that the greater part of the elements, 68.17%, are used to model the 3D components (air cavities, trim panel, air cloak). Furthermore, elements must have Jacobian determinant ratio as close as possible to 1, so they do not have to be too irregular. Only 3520 elements (0.27%) have Jacobian determinant ratio lower than 0.7.

The mesh quality is reported in Fig. 10. All meshes are above their criteria except the meshes of trim panel, overheads and windows, for the maximum frequency in the analysis (300 Hz). Windows have a value of 6.87, which is still acceptable (the results for this component could have a maximum inaccuracy of 1.85%). The overheads are unchanged to maintain element size similar to the elements size of the external shell. Finally, the trim panel mesh, though below 3 elements per wavelength, does not cause a drop in accuracy.

Each analysis takes almost one hour per frequency to complete, including the creation of the structure, the time to solve the equations and save the results.



(b)

Figure 5: Dimensions of the model in mm. (a) Front view (b) Lateral view.

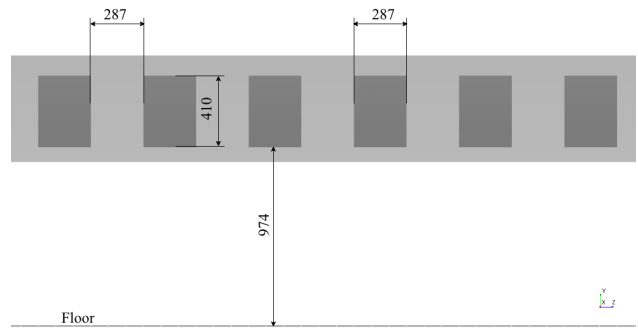


Figure 6: Windows sizes in mm.

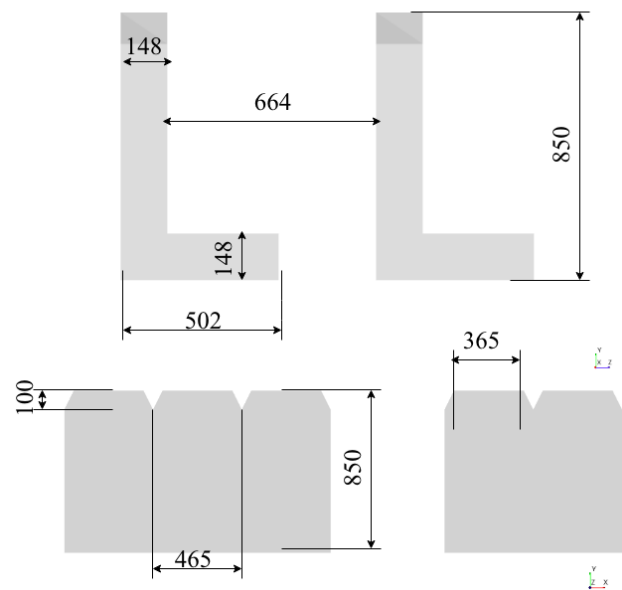


Figure 7: Seats sizes and layout in mm.

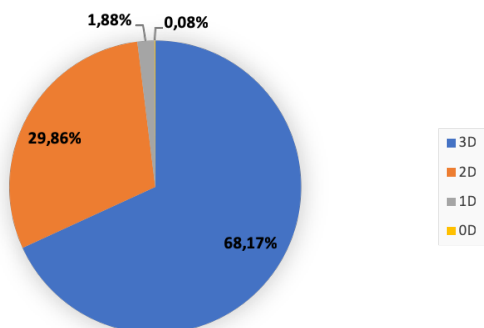


Figure 8: Distribution of elements based on their dimension.

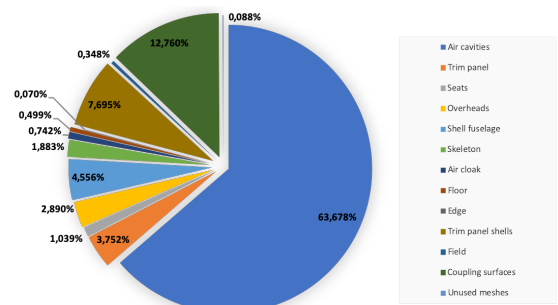


Figure 9: Distribution of elements based on their dimension.

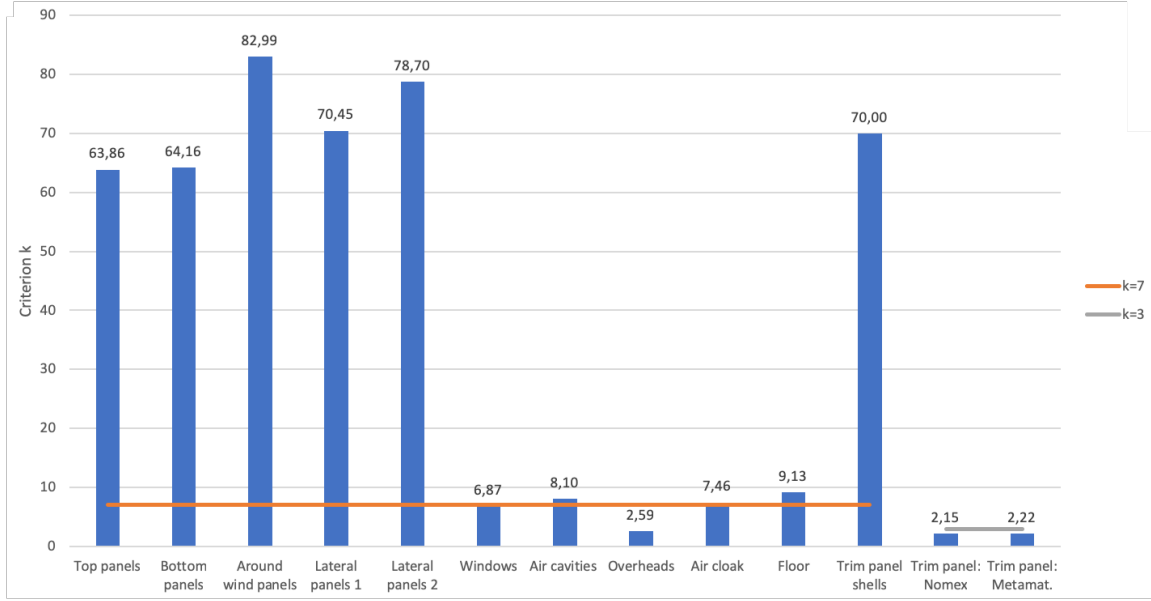


Figure 10: Elements per wavelength for each component at 300 Hz.

2.2 Pressure loads

The loads calculated by CIRA (*Centro Italiano di Ricerca Aerospaziale*) represent the pressure field generated at blade passage frequency (BPF) by two 8-blade propellers rotating clock-wise with 20 degrees relative phase angle (Fig. 11) in the first three harmonics, that occur at 100 Hz, 200 Hz and 300 Hz according to the number of blades and propeller rotation per minute (RPM) at cruise velocity. The aerodynamic pressure has been calculated using Blade element momentum theory (BEMT) and then, from the aerodynamic pressure, the acoustic pressure distribution over the fuselage external skin has been computed using a FW-H (Ffowcs Williams and Hawkings) approach. The pressure field is calculated on mesh of 9792 nodes that represent the aircraft fuselage. The pressure is a complex value in Pascal, function of spatial coordinates x , y and z (and of frequency f).

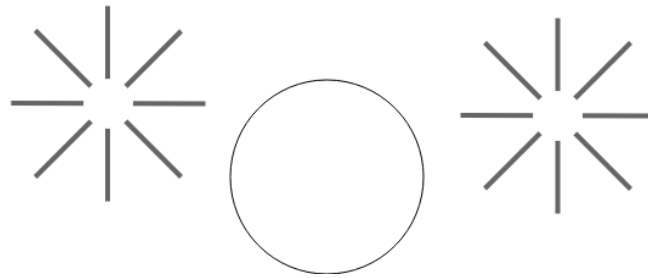


Figure 11: 8-blade propeller configuration.

The pressure loads are applied to the fuselage through a virtual air cloak with a pressure boundary condition. This virtual cloak is modeled as a fluid (3D elements) component with a thickness of 1 mm (two nodes on the thickness). On this virtual cloak the loads are applied as a one-dimensional field where pressure, as a complex number, is defined on the nodes. For the internal nodes the propeller loads are applied, while for the external node a zero pressure is defined. The physical and virtual fuselages are linked through an interface where the first coupling surface is the physical fuselage (bottom and top fuselage, lateral panels, window belt, windows and removed windows) and the second is the virtual air

cloak surface. During the meshing process, particularly running the merge nodes function, 136 nodes are eliminated as duplicates (one for every circle that composes the virtual air cloak), and, consequently, the corresponding loads, so 9656 nodes remain.

The loads are reported in Fig. 12 for 100 Hz, Fig. 13 for 200 Hz and Fig. 14 for 300 Hz both the real part and imaginary part in Pascal.

Finally the fuselage is bound by zero displacements and rotations boundary condition.

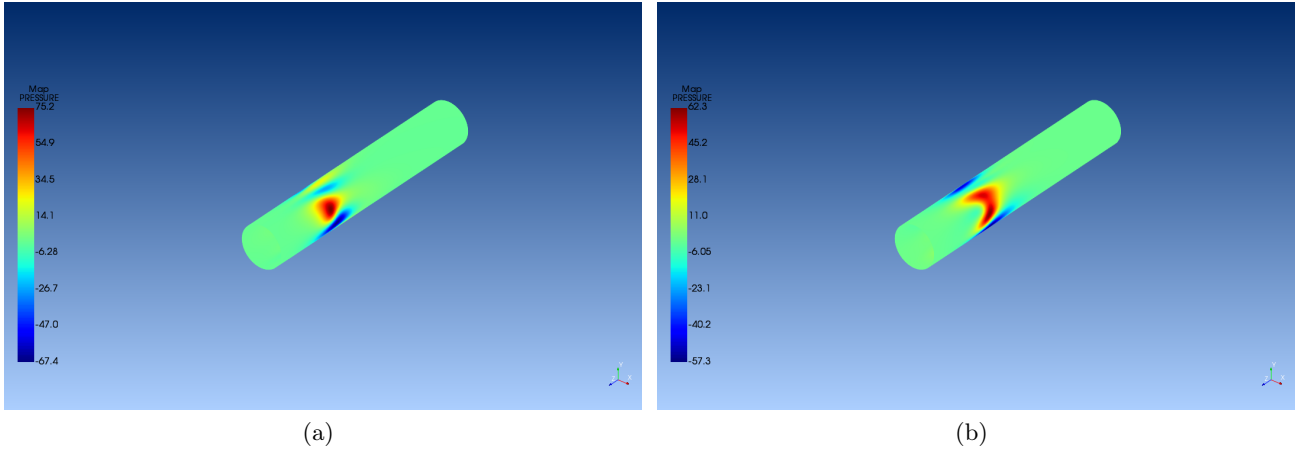


Figure 12: Pressure loads [Pa] for the first tonal frequency 100 Hz. (a) Real part. (b) Imaginary part.

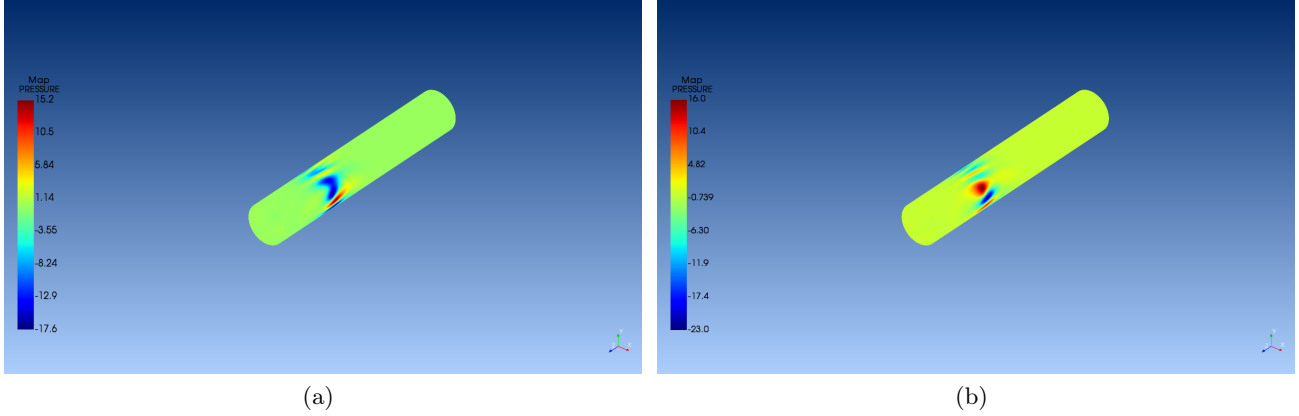


Figure 13: Pressure loads [Pa] for the second tonal frequency 200 Hz. (a) Real part. (b) Imaginary part.

2.3 Acoustic solutions

In this work, we will consider a baseline configuration of the regional aircraft without any acoustic treatments, in which the trim panels are made of sandwich material with Nomex core and fiberglass/epoxy skins. This is the reference model that the new cabin configuration is related to in order to evaluate the noise reduction.

Nomex is an orthotropic material with only structural purpose; its characteristics are reported in Tab. 1. The fiberglass skin properties are reported in Tab. 1. The trim panel core (Nomex) has a thickness

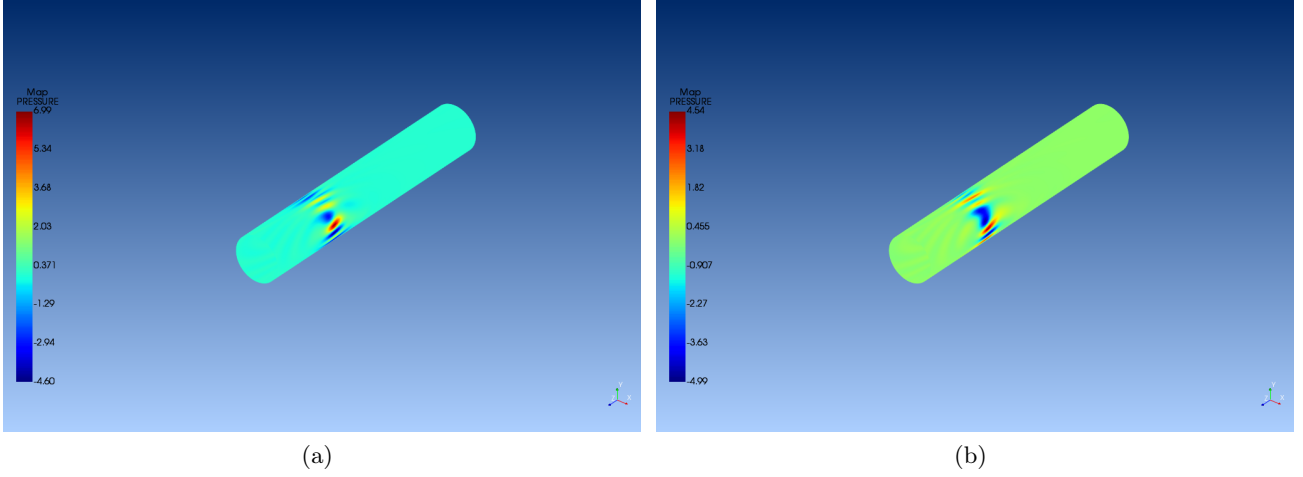


Figure 14: Pressure loads [Pa] for the third tonal frequency 300 Hz. (a) Real part. (b) Imaginary part.

of 6 mm, while the plates have a thickness of 0.48 mm each, with a single layer thickness of 0.24 mm and an orientation of the fibers equal to 0° and 90° . Density of Nomex is equal to 48 kg/m³ and the plate density is equal to 1950 kg/m³.

Table 1: Nomex and fiberglass/epoxy properties.

	Nomex	Fiberglass
E_x [Pa]	1.0E+05	2.0E+10
E_y [Pa]	1.0E+05	2.0E+10
E_z [Pa]	9.0E+07	3.6E+09
ν_{xy}	9.9E-01	1.3E-01
ν_{xz}	2.0E-04	2.7E-01
ν_{yz}	2.0E-04	2.7E-01
G_{xy} [Pa]	1.0E+05	4.0E+09
G_{xz} [Pa]	1.5E+07	4.3E+09
G_{yz} [Pa]	3.1E+05	4.3E+09

Table 2: Window isotropic materials (tempered glass and plexiglass) properties.

	Tempered glass	Plexiglass
E [Pa]	4.00E+10	2.79E+09
ν	2.20E-01	3.70E-01
ρ [kg/m ³]	2.20E+03	1.18E+03

The chosen metamaterial is a melamine foam with cylindrical inclusions of aluminium with volume fraction of 0.015. Its frequency dependent properties are reported in Tab. 3 and calculated by D'Amico et al. [20]. The advantages of using melamine (formaldehyde-melamine-sodium bi-sulfite copolymer) are high sound absorption capacity, low weight, good thermal insulation properties and flexibility at very low temperature; moreover, this material is fireproof. Aluminium is used because of its proven efficiency in aeronautics. The total density of this metamaterial is very similar to the density of Nomex: 48.38 kg/m³ for the metamaterial instead of 48.00 kg/m³ for the Nomex. The two fiberglass plates and the thickness of the core remain the same.

The second acoustic solution is to have the fuselage and the trim panel without windows. The windows are made of tempered glass and plexiglass (Tab. 2) and they have a thickness of 3 mm per layer. The air between the two materials of the windows is neglected, although it would have a positive effect on sound reduction.

The whole fuselage is made of composite materials and the overheads of PVC (polyvinyl chloride). The seat material is not explicitly defined but a normalized impedance value has been associated to the shell

Table 3: Characteristics of the metamaterial composed by a melamine foam with cylindrical inclusions of aluminium with volume fraction of 0.015.

Frequency [Hz]	100		200		300	
	Im	Re	Im	Re	Im	Re
E_x [Pa]	1.541E+06	5,182E+03	1.549E+06	6.344E+03	1.555E+06	7.115E+03
E_y [Pa]	2.883E+05	2.467E+03	2.899E+05	3.020E+03	2.910E+05	3.387E+03
E_z [Pa]	1.014E+09	2.040E+03	1.014E+09	2.497E+03	1.014E+09	2.801E+03
ν_{xy}	2.194E-01	8.574E-03	2.194E-01	8.574E-03	2.194E-01	8.574E-03
ν_{xz}	-4.973E-01	1.000E-07	-4.973E-01	1.000E-07	-4.973E-01	1.000E-07
ν_{yz}	4.274E-01	1.000E-07	4.274E-01	1.000E-07	4.274E-01	1.000E-07
G_{xy} [Pa]	1.064E+05	1.174E+03	1.069E+05	1.437E+03	1.073E+05	1.612E+03
G_{xz} [Pa]	1.306E+05	1.464E+03	1.313E+05	1.792E+03	1.318E+05	2.010E+03
G_{yz} [Pa]	1:098E+05	1.231E+03	1.104E+05	1.507E+03	1.108E+05	1.690E+03

elements on the boundaries of the seats that is frequency dependent, Fig 15.

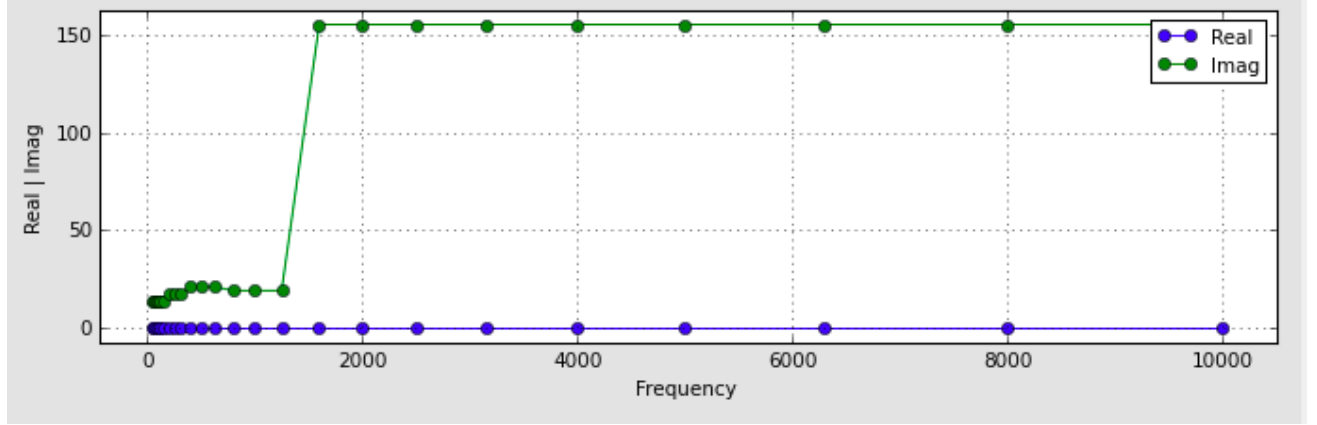


Figure 15: Non-normalized impedance as a function of frequency.

2.4 Analysis and solver

A direct frequency response analysis is performed in order to obtain the sound pressure level inside the cabin. This analysis computes the response of an acoustic system to specific excitation in physical coordinates. The following system of equations must be solved for various pulsations $\omega = 2\pi f$ (f is the frequency)

$$(\mathbf{K} + i\omega\mathbf{C} - \omega^2\mathbf{M}) \cdot \mathbf{x}(\omega) = \mathbf{F}(\omega) \quad (1)$$

in which $\mathbf{x}(\omega)$ is an unknown vector. The analysis is run for the three tonal frequencies of the pressure loads: 100 Hz, 200 Hz and 300 Hz. At each frequency, the corresponding load is applied. The analysis is performed with both the baseline cabin configuration and the innovative configurations exploiting the acoustic treatments. An overview of the analysis is shown in Tab. 4.

The MUMPS solver in Actran has been chosen to find the solution of direct frequency response. This solver is based on LU decomposition of the following algebraic system:

$$\mathbf{Z}\mathbf{x} = \mathbf{B} \quad (2)$$

Table 4: Analysis overview.

Frequency [Hz]	Trim panel material	Windows
100	Nomex	Yes
		No
	Metamaterial	Yes
		No
200	Nomex	Yes
		No
	Metamaterial	Yes
		No
300	Nomex	Yes
		No
	Metamaterial	Yes
		No

and it assembles \mathbf{Z} matrix and then factorizes it to find the lower \mathbf{L} and upper \mathbf{U} matrix:

$$\mathbf{Z} = \mathbf{L}\mathbf{U} . \quad (3)$$

This method is called sequential approach and, apart from MUMPS, it includes SPARSE, CG_ILU and PARDISO solvers. MUMPS could be also based on frequency and azimuthal order parallelism computation, domain parallelism computation and matrix parallelism computation. MUMPS (multifrontal massively parallel solver) is used with a sub-solver SCALAPACK to assemble interfaces.

This solver has been preferred to KRYLOV solver because this last solver works better with materials and boundary conditions that have a simple relation with the frequency. It is not the case of metamaterials or impedance boundary conditions.

2.5 Output requests

Sound pressure is evaluated in five sets of points (output of Frequency Response Function analysis). The five sets represent the head position of seated passenger, at a height of 1.20 m from the floor and disposed above the seats. Furthermore, a field map at 1.20 m from the floor inside the cabin (same heights of the five sets) is created to visualize the pressure map.

3 Results

3.1 Modal extraction

Initially, a modal extraction of the model was run in Actran on the fuselage structure without air cavities, seats and external loads for the baseline model (trim panel in Nomex and windows) as a validation of FEM model. The obtained modes prove to be very complex because of the presence of the bars between the fuselage panels and the trim panel. The first mode (displacements and rotations) for fuselage panels is reported in Fig. 16 and in Fig. 17 at frequency of 0.208 Hz.

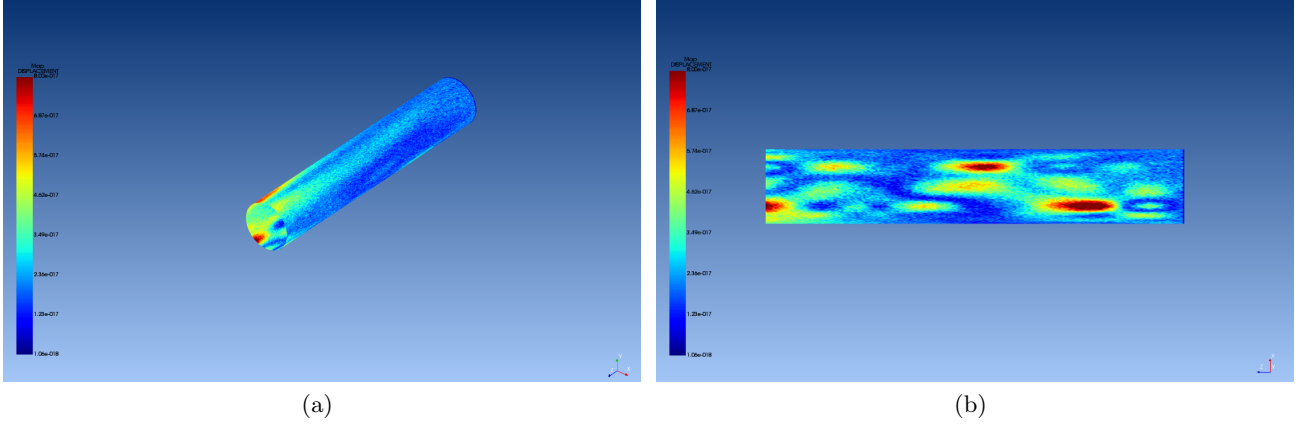


Figure 16: First mode displacements [m] at 0.208 Hz. (a) Perspective view. (b) View from above.

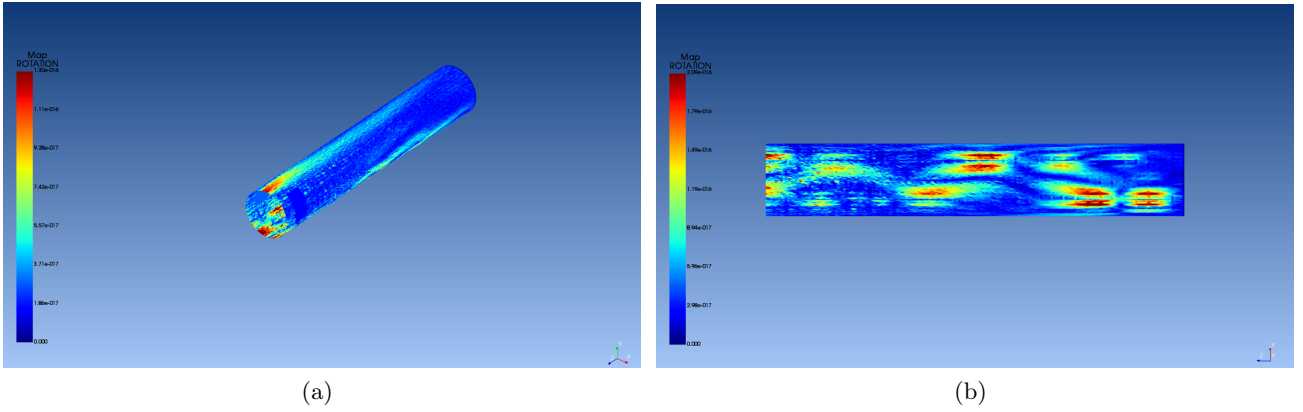


Figure 17: First mode rotations [°] at 0.208 Hz. (a) Perspective view. (b) View from above.

3.2 Vibroacoustic results

The results are calculated in terms of SPL (Sound Pressure Level) and OASPL (Overall Sound Pressure Level) in dBA. The SPL is defined as:

$$SPL = 20 \cdot \log_{10} \frac{p}{p_{ref}} \text{ dB} \quad (4)$$

where $p_{ref} = 20 \mu\text{Pa}$ for air and p is the pressure in Pascal that depends on frequency. The OASPL is expressed as:

$$OASPL = 20 \cdot \log_{10} \frac{\sqrt{\int_{f_{min}}^{f_{max}} p^2 dp}}{p_{ref}} \text{ dB} \quad (5)$$

where f_{min} and f_{max} are minimum and maximum frequency on which the pressure p is calculated.

The weights of dBA for 100 Hz, 200 Hz and 300 Hz are respectively -19.1451, -10.8472 and -7.0546. The SPL is calculated as mean of the five sets of FRF points (microphones), so as a mean of sound pressure perceived by seated passenger (1.20 m from the floor). Then the OASPL is the weighted mean of SPL on frequency. The results refer to the twelve analyses performed, Tab. 4. Pressure maps are obtained at 1.20 m from the floor. As expected, independently from the acoustic solution, the SPL decrease with

the frequency. Indeed, the pressure load magnitude decreases from 100 Hz to 300 Hz. Finally, for higher frequencies (200 Hz and 300 Hz) it is possible to define a noisier region near the propellers.

An overview of the results is shown in Fig. 18. The SPL maps in dBA for the three tonal frequencies and for each analysis are reported from Fig. 19 to Fig. 24.

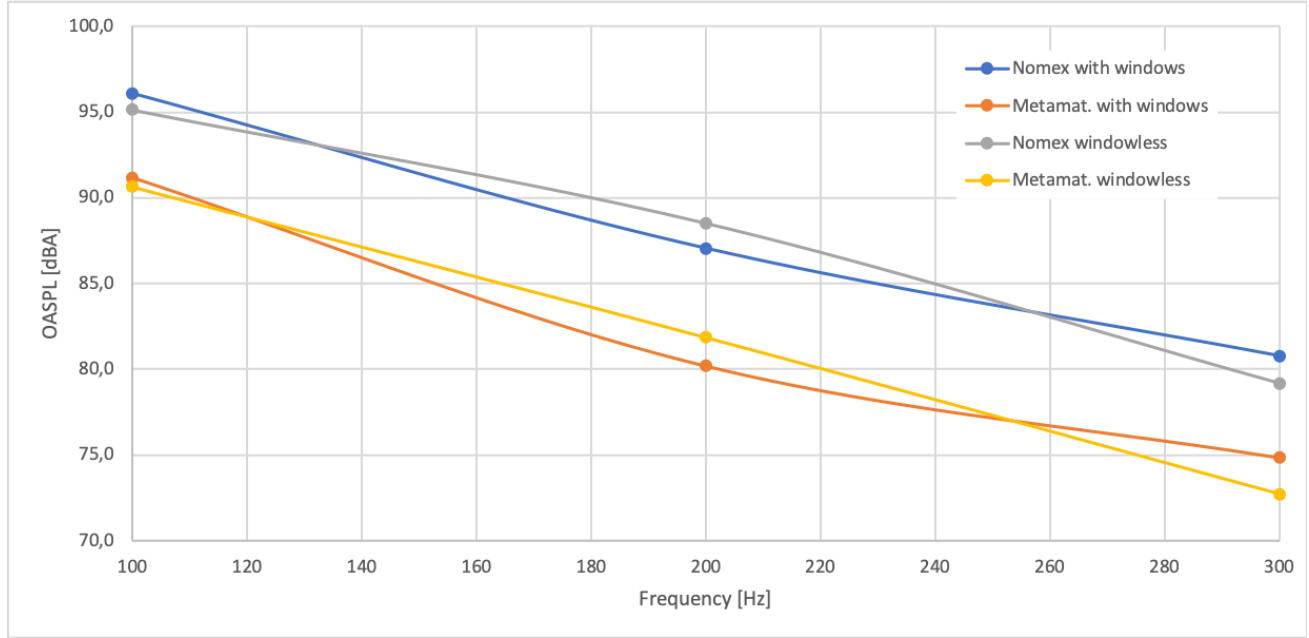


Figure 18: The results, in terms of SPL [dBA] for each tonal frequency [Hz], are compared.

3.3 Trim panel in metamaterial

The OASPL on the three frequencies is equal to 87.7555 dBA for a trim panel made of Nomex, it is equal to 81.6033 dBA for a trim panel made of metamaterial. The OASPL, for a windowless aircraft, on the three frequencies is equal to 87.8538 dBA for a trim panel made of Nomex, it is equal to 81.7751 dBA for a trim panel made of metamaterial.

The trim panel made of metamaterial is acoustically more efficient than a trim panel made of Nomex. In fact, there is a mean reduction of 6.1522 dBA, equal to 7.01% of total OASPL. The sound pressure is almost halved, falling from 0.488 Pa to 0.241 Pa. For a windowless configuration, the effect of the metamaterial is similar to a conventional aircraft.

3.4 Windowless configuration

The removal of windows does not show a general reduction or increase in OASPL. Indeed, the OASPL increases for the trim panel of Nomex of 0.0983 dBA, by almost 0.11%, while for the trim panel made of metamaterial by almost 0.21% (0.1718 dBA). Furthermore, the noise reduction (or increase) due to the absence of windows strongly depends on frequency with a non-monotone behavior. In fact, the transmission loss of these two materials strongly depend on frequency, as shown in Fig. 25(a) and (b). To obtain the transmission loss of these two materials an experimental test is simulated in Actran, using two panels with same thickness as the fuselage and the windows respectively and a monopolar acoustic source, Fig. 25(c). A similar analysis was carried out for an aluminum panel.

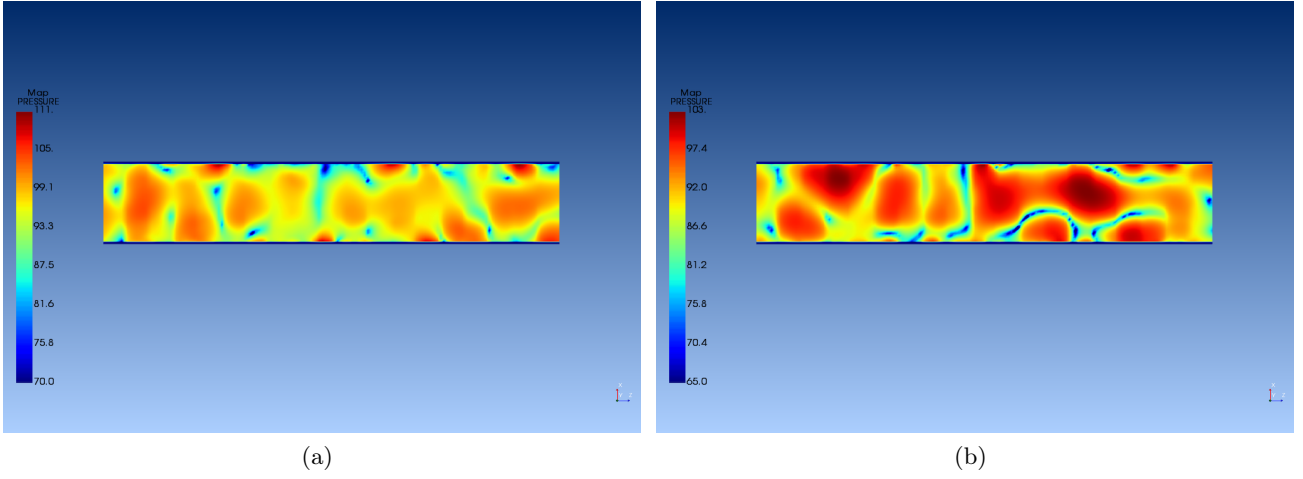


Figure 19: SPL maps at 100 Hz in dBA for a configuration with windows. (a) Nomex. (b) Metamaterial.

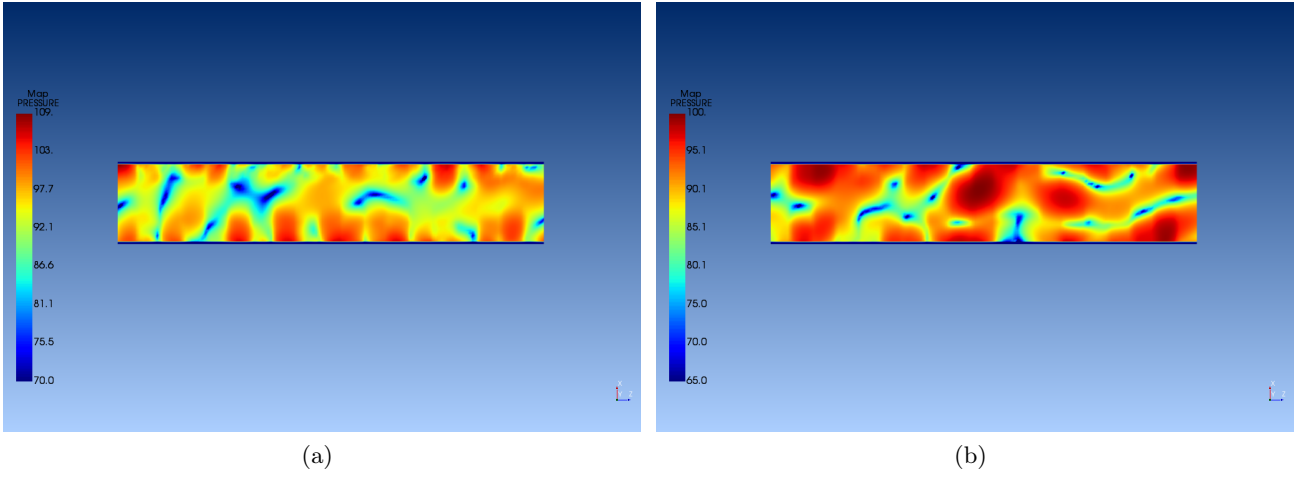


Figure 20: SPL maps at 100 Hz in dBA for a windowless configuration. (a) Nomex. (b) Metamaterial.

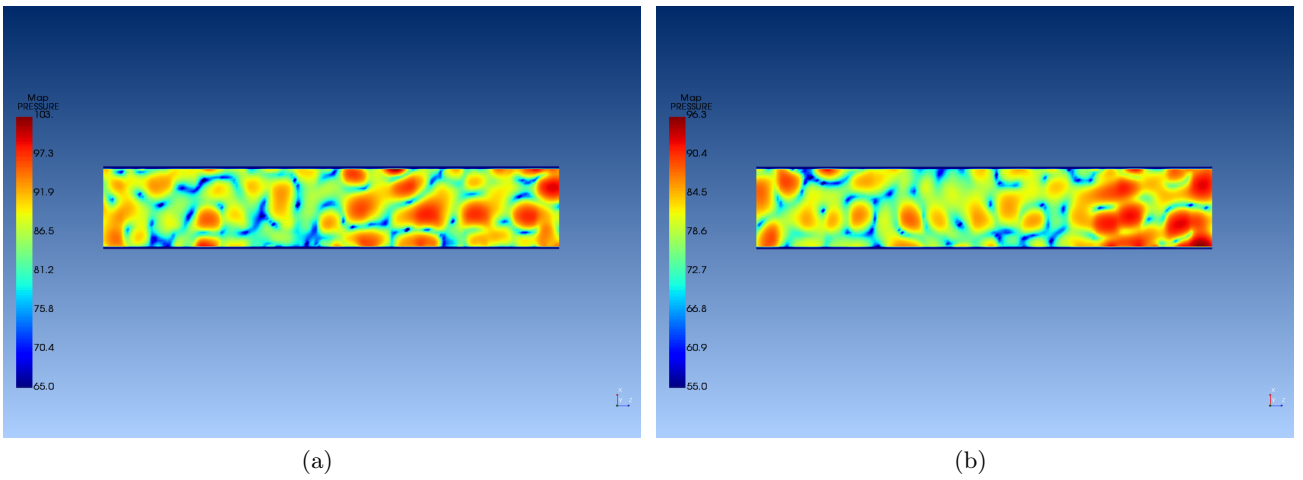


Figure 21: SPL maps at 200 Hz in dBA for a configuration with windows. (a) Nomex. (b) Metamaterial.

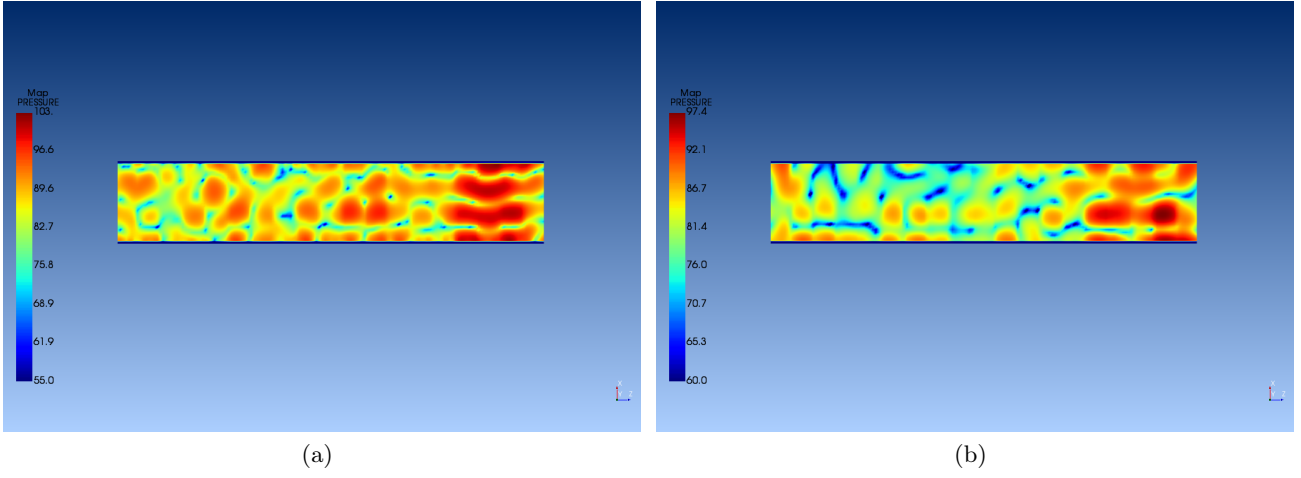


Figure 22: SPL maps at 200 Hz in dBA for a windowless configuration. (a) Nomex. (b) Metamaterial.

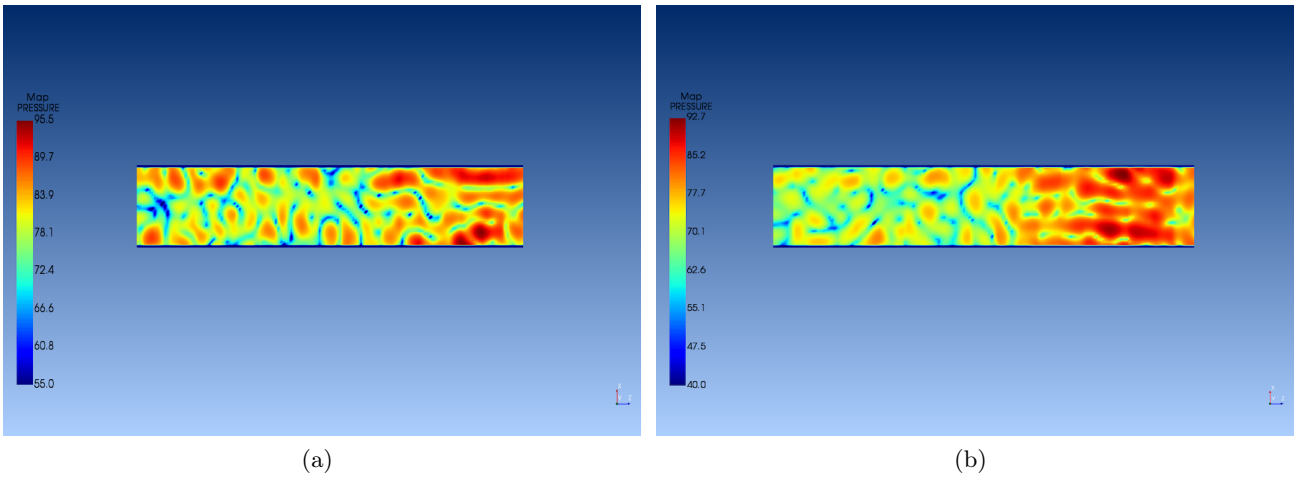
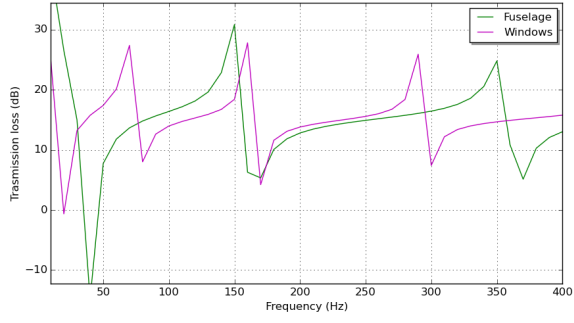


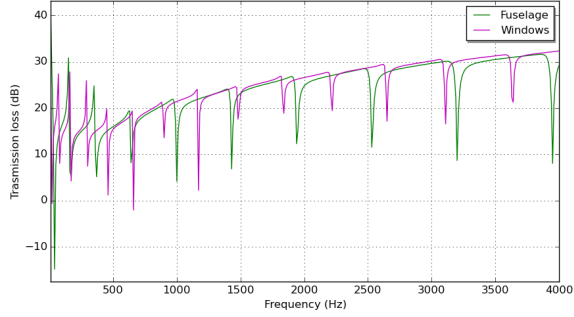
Figure 23: SPL maps at 300 Hz in dBA for a configuration with windows. (a) Nomex. (b) Metamaterial.

(a)

Figure 24: SPL maps at 300 Hz in dBA for a windowless configuration. (a) Nomex. (b) Metamaterial.



(a)



(b)

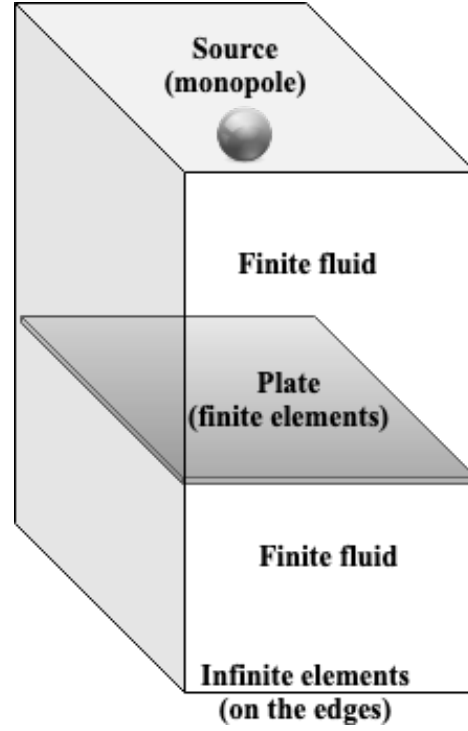


Figure 25: Transmission loss [dB] due to the fuselage skin near the windows (green) and due to the windows (magenta). (a) From 10 to 400 Hz. (b) From 10 to 4000 Hz. (c) Model to evaluate the transmission loss of the fuselage and window materials.

4 Conclusions

This work demonstrates the acoustic efficiency of metamaterials for a regional turboprop aircraft, considering, unlike other works, an almost complete fuselage FEM model and realistic pressure loads. In particular, a trim panel made of metamaterial leads to a significant reduction in cabin noise, with a consequential increase in passenger comfort. Although the windowless configuration, from an acoustic point of view, does not exploit significant advantages like it does in terms of fuel consumption and emission reduction.

The following remarks, derived from the numerical results, are obtained:

- the performed analysis strongly depends on the trim panel material, therefore optimizing the metamaterials (host material, inclusion size and material, thickness) could lead to better results in terms of noise reduction;
- sound pressure tends to increase with frequency, while the pressure loads have the opposite behavior;
- the sound pressure level distribution in the cabin seems to assume a more coherent structure with the frequency increases; in fact, at 200 Hz and 300 Hz the loudness region is near the propellers plane, while at 100 Hz the distribution is more chaotic;
- using composite material for fuselage panels, it leads to worse acoustic insulation than using traditional aluminum panels. It results that the windows have a similar insulation capability to that

of the fuselage panel, undermining the possible acoustic advantages of a windowless configuration.

Besides numerical results and considerations, the aim of this work is to lay the foundation for further studies; in particular, the computational model could be used to optimize the metamaterials. Furthermore, different configurations could be studied, using other active or passive acoustic solutions. It is also important to perform a structural analysis on the trim panel with metamaterial to satisfy safety and legislative requirements. Analysis at high frequencies must also be performed to evaluate the metamaterials efficiency outside their nominal design range.

For the windowless configuration an analysis on a wider and higher frequency range could better determine if the sound pressure level decreases or not due to the removal of windows.

Beyond these technological considerations, the proposed concepts could provide a contribution to the global strategies of reducing noise in the cabin and increasing passenger comfort using innovative materials and configurations.

References

- [1] J W S Rayleigh. *The Theory of Sound*. Macmillan & Co., London, 1877.
- [2] L L Beranek. *Noise Reduction*, page 258. McGraw-Hill Book Company Inc., NY, 1960.
- [3] L L Beranek. The noisy dawn of the jet age. *Sound and Vibration Magazine*, January 2007.
- [4] Mathias Basner, Wolfgang Babisch, Adrian Davis, Mark Brink, Charlotte Clark, Sabine Janssen, and Stephen Stansfeld. Auditory and non-auditory effects of noise on health. *Lancet*, 383, 10 2013.
- [5] R H Nichols, H P Jr Sleeper, R L Jr Wallace, and H L Ericson. Acoustical materials and acoustical treatments for aircraft. *Journal of the Acoustical Society of America*, 19(3):428–443, 1947.
- [6] W Dobrzynski. Almost 40 years of airframe noise research: What did we achieve? *Journal of Aircraft*, 47(2):353–367, 2010.
- [7] N Sui, X Yan, T-Y Huang, J Xu, F-G Yuan, and Y Jing. A lightweight yet sound-proof honeycomb acoustic metamaterial. *Applied Physics Letters*, 106:171905, 2015.
- [8] R Liu, C Ji, Z Zhao, and T Zhou. Metamaterials: Reshape and rethink. *Engineering*, 1(2):179–184, 2015.
- [9] C Caloz. Perspectives on em metamaterials. *Materials Today*, 12(3):12–20, 2009.
- [10] P Alitalo and S Tretyakov. Electromagnetic cloaking with metamaterials. *Materials Today*, 12(3):22–29, 2009.
- [11] R Grimberg. Electromagnetic metamaterials. *Materials Science and Engineering: B*, 178(19):1285–1295, 2013.
- [12] K Fan and W J Padilla. Dynamic electromagnetic metamaterials. *Materials Today*, 18(1):39–50, 2015.
- [13] A A Zadpoor. Mechanical meta-materials. *Materials Horizon*, 3(5):371–381, 2016.
- [14] C Coulaïs, D Sounas, and A Alù. Static non-reciprocity in mechanical metamaterials. *Nature*, 542:461–464, 2017.

- [15] K Bertoldi, V Vitelli, J Christensen, and M van Hecke. Flexible mechanical metamaterials. *Nature Reviews Materials*, 2(17066), 2017.
- [16] S. Chen, Y. Fan, Q. Fu, H. Wu, Y. Jin, J. Zheng, and F. Zhang. A review of tunable acoustic metamaterials. *Applied Sciences*, 8:1480, 08 2018.
- [17] X. Zhang, J. Mei, M. Yang, N H Chan, and P. Sheng. Membrane-type acoustic metamaterial with negative dynamic mass. *Physical review letters*, 101:204301, 12 2008.
- [18] J. Mei, G. Ma, M. Yang, Z Yang, W Wen, and P. Sheng. Dark acoustic metamaterials as super absorbers for low-frequency sound. *Nature communications*, 3:756, 03 2012.
- [19] L. Zheng, Y. Wu, X. Ni, Z. Chen, M. Lu, and Y. Chen. Acoustic cloaking by a near-zero-index phononic crystal. *Applied Physics Letters*, 104:161904–161904, 04 2014.
- [20] A.G. De Miguel M. Filippi A. Pagani E. Carrera M. Cinefra, G. D’Amico. Numerical evaluation of transmission loss in acoustic metamaterials for aeronautical applications.
- [21] E. Yuksel, G. Kamci, and I. Basdogan. Vibro-acoustic analysis of a vehicle integrated with design of experiments methodology using three performance criteria. 06 2019.
- [22] G. Accardo, B. Peeters, F. Bianciardi, K. Janssens, M. El-kafafy, D. Brandolisio, and M. Martarelli. Experimental acoustic modal analysis of an automotive cabin. *Sound and Vibration*, 49:10–18, 05 2015.
- [23] M. Cinefra, S. Passabí, and E. Carrera. Fem vibroacoustic analysis in the cabin of a regional turboprop aircraft. *Advances in Aircraft and Spacecraft Science*, 5:477–498, 07 2018.
- [24] M. Cinefra and G. Petrone. Sea analysis in the cabin of a regional turboprop with metamaterial lining panels. 01 2019.
- [25] F. Franco, S. De Rosa, and T. Polito. Finite element investigations on the vibroacoustic performance of plane plates with random stiffness. *Mechanics of Advanced Materials and Structures*, 18:484–497, 10 2011.
- [26] G. Petrone, V. D’Alessandro, F. Franco, and S. De Rosa. Numerical and experimental investigations on the acoustic power radiated by aluminium foam sandwich panels. *Composite Structures*, 118:170–177, 12 2014.
- [27] Arunkumar M P, Jeyaraj P, Gangadharan K V, and Lenin M C. Influence of nature of core on vibro acoustic behavior of sandwich aerospace structures. *Aerospace Science and Technology*, 56, 07 2016.
- [28] V. D’Alessandro, G. Petrone, F. Franco, and S. De Rosa. A review of the vibroacoustics of sandwich panels: Models and experiments. *Journal of Sandwich Structures and Materials*, 15:541–582, 09 2013.
- [29] V. Cutanda Henriquez, P. R. Andersen, and J. Søndergaard Jensen. A numerical model of an acoustic metamaterial using the boundary element method including viscous and thermal losses. *Journal of Computational Acoustics*, 11 2016.
- [30] S. Bagassi, F. Lucchi, and F. Persiani. Aircraft preliminary design: a windowless concept. In *5th CEAS 20015 Proceedings*, 2015.

- [31] C. Berth, G. Huttig, and O. Lehmann. Research on integrated collimated cockpit visual and flight information system. In *26th ICAS 2008 Proceedings*.
- [32] J. Zaneboni and B. Saint Jalmes. Aircraft with a cockpit including a viewing surface for piloting which is at least partially virtual. In *U.S. patent no. 2014/0180508*. March 6 2014.
- [33] H. R. Liebeck. Design of the blended wing body subsonic transport. *Journal of Aircraft - J AIRCRAFT*, 41:10–25, 01 2004.
- [34] Z Van Der Voet, Francois Geuskens, T J. Ahmed, B Ninaber Van Eyben, and Adriaan Beukers. Configuration of the multibubble pressure cabin in blended wing body aircraft. *Journal of Aircraft*, 49:991–1007, 07 2012.
- [35] S. Bagassi, F. Lucchi, and M. C. Moruzzi. The windowless concept: preliminary design of short-medium range windowless aircraft. In *24th AIDAA 2017 Proceedings*, 2017.
- [36] S. Bagassi, F. Lucchi, and M. C. Moruzzi. Preliminary design of a long range windowless aircraft concept. In *31th ICAS 2018 Proceedings*, 2018.